

Dependence of Magnetic Properties on the Growth Conditions of MnGaN Grown by rf N Plasma Molecular Beam Epitaxy

Muhammad B. Haider¹, Costel Constantin¹, Hamad Al-Britthen¹, Gabriel Caruntu², Charles J. O'Connor², and Arthur R. Smith*¹

¹ Department of Physics and Astronomy, Ohio University, Athens, OH 45701

² Advanced Materials Research Institute, University of New Orleans, New Orleans, LA 70148

Received zzz, revised zzz, accepted zzz

Published online zzz

PACS 75.50.Pp, 81.15.Hi, 61.10.Nz, 61.14.Hg

MnGaN has been grown by radio frequency N plasma-assisted molecular beam epitaxy. MnGaN samples were grown on MOCVD GaN(0001)/sapphire(0001) at substrate temperature of 550 °C under different Ga/N flux ratios leading to 4 different growth regimes: N-rich, slight metal-rich, metal-rich, and Ga-rich. It is found that in the case of MnGaN, Mn incorporation and hence magnetic properties clearly depend on the growth conditions. Briefly, it is found that the N-rich conditions give a sample with much larger magnetization compared to the other samples. Slight metal-rich and metal-rich grown samples have very little magnetization. Finally, Ga-rich grown samples have intermediate level of magnetization. Possible origins of the magnetization are discussed. Ga-rich magnetization is attributed to accumulates, but N-rich magnetization is attributed to carrier-mediated ferromagnetism and/or ferromagnetism due to clusters.

Copyright line will be provided by the publisher

1 Introduction

For the last two decades, spintronics (spin-based electronics) has attracted much attention where not only charge but also spin degree of freedom of electron can be used. For this purpose ferromagnetic(FM) metals were deposited on the semiconductor surfaces but it was thought that polarized spin injection could be limited because of the scattering centers at the FM and semiconductor interface. A dilute magnetic semiconductor(DMS) is an attractive alternative because DMS can have an ideal interface with other semiconductors. Recently, GaMnAs dilute magnetic semiconductor(DMS) has been shown to function as a spin injector; however the Curie temperature (T_C) for this material was only 110 K.[1]

Sato *et al.* have predicted, based on first-principles calculation in the mean field approximation, that MnGaN DMS can exhibit ferromagnetism above room temperature.[2] There are several reports about the growth and ferromagnetism of MnGaN DMS systems.[3, 4, 5, 6] But the reported Curie temperature of these materials varies from 10K to 940K. Moreover, there could be various configurations of Mn, including in the form of 1) magnetic accumulates (or precipitates); 2) Mn_xN clusters; and 3) Mn ions. So this remains an open issue how the Curie temperature, accumulation (precipitation), Mn_xN clustering, and Mn ion formation, depend on the growth conditions. In this paper, we report a systematic growth study of MnGaN and discuss the effect of different growth conditions on the magnetic properties of MnGaN.

2 Experimental

Transition metal (TM) doped GaN growth was performed in a molecular beam epitaxy(MBE) chamber dedicated to the growth of nitrides. In the growth chamber, solid state effusion cells are used for Ga and

* Corresponding author: e-mail: smitha2@ohio.edu, Phone: +01 740 597 2576, Fax: +01 740 593 0433

Mn sources. RF plasma is used for nitrogen with N_2 as the source gas. During the MnGaN growth, chamber background pressure is set at 9.1×10^{-6} Torr. Growth is monitored *in situ* by reflection high energy electron diffraction (RHEED).

MnGaN samples were grown on MOCVD GaN(0001)/Sapphire(0001) substrates at sample temperature of 550 °C with different Ga/N flux ratios ($R_{Ga:N}$) ranging from 0.7 to 1.46 with constant N flux. Mn/N flux ratio ($R_{Mn:N}$) was kept constant at ~ 0.07 . First a 30 nm thick GaN buffer layer was grown, then ~ 0.3 - $0.6 \mu\text{m}$ thick main MnGaN layer was grown, the growth was finished with a 30 nm thick GaN cap layer.

After removal from the growth chamber, the samples were characterized by a variety of techniques. Here we report on the results of *ex-situ* atomic force microscopy (AFM) measurements which are correlated very well with the RHEED patterns; furthermore, the magnetic properties of the samples were measured using a superconducting quantum interference device (SQUID). Zero field cooled and field cooled measurements were performed after demagnetizing the sample. Samples were cooled to a temperature of 5K under zero magnetic field then samples were heated slowly to room temperature under the magnetic field of 200 Oe applied parallel to the plane of the film and magnetization of the sample was recorded at each interval. Then samples were cooled down to 5K in a similar fashion in the presence of a magnetic field of 200 Oe and data was recorded.

3 Results and Discussions

3.1 Modes of Growth

We show that there are 4 distinguishable modes of growth as a function of Ga flux: N-rich, metal-rich, and Ga-rich. The Metal-rich growth mode can further be divided into slight metal-rich and heavy metal-rich growth modes. These modes are distinguished by their RHEED patterns and have distinctly different surface morphology as seen in AFM images. For comparison overall grey scale is shown on the right hand corners of the AFM images.

Qualitatively, these growth conditions can be defined as that under N-rich conditions, there are more surface N atoms than surface Ga and Mn atoms. Metal-rich growth conditions can be defined such that there are more surface metal atoms (Ga+Mn) than surface N atoms. Under Ga-rich conditions, there are more surface Ga atoms than surface N atoms. The ratio of the chemical species present on the surface (e.g., Ga/N) is a function of Ga, Mn and N fluxes, but it is not directly equal to the ratios of those flux values. The reason is that the sticking coefficient of different species varies as a function of the chemical potential of the surface, which in turn determines the surface structure which affects the growth mode. For example, under Ga-rich conditions in which the interaction is between Ga and weakly bound Ga on the surface, the sticking coefficient of Ga will be smaller than under Ga-poor conditions where the interaction of Ga adatoms is not only with surface Ga but also with other species (Mn and N) present on the surface. In the following discussion, we will describe the results in terms of the flux ratios. Interestingly, it is shown below that each of these modes also corresponds to different magnetic properties.

3.1.1 N-rich Growth Mode

Shown in Fig. 1(a,b) is the RHEED pattern and AFM image of the MnGaN(0001) sample (MnGaN-1) grown under N-rich conditions ($R_{Ga:N} = 0.76$). The RHEED pattern of the sample is spotty which is an indication of the 3D growth mode, and this is confirmed by the $5 \mu\text{m} \times 5 \mu\text{m}$ AFM image (with gray scale of 326 Å and rms roughness of 57 Å inside the box area) which shows a rough surface consisting of small hillocks but no other noticeable features. This kind of rough surface/3D growth mode is also observed for growth under N-rich conditions without Mn.[7, 8, 9] The N-rich growth mode for GaN(0001) has been explained as due to N accumulation on the surface and loss of Ga, which reduces the surface diffusion for both Ga and N atoms. Mn does not appear to remove this effect. Rutherford backscattering (RBS) has

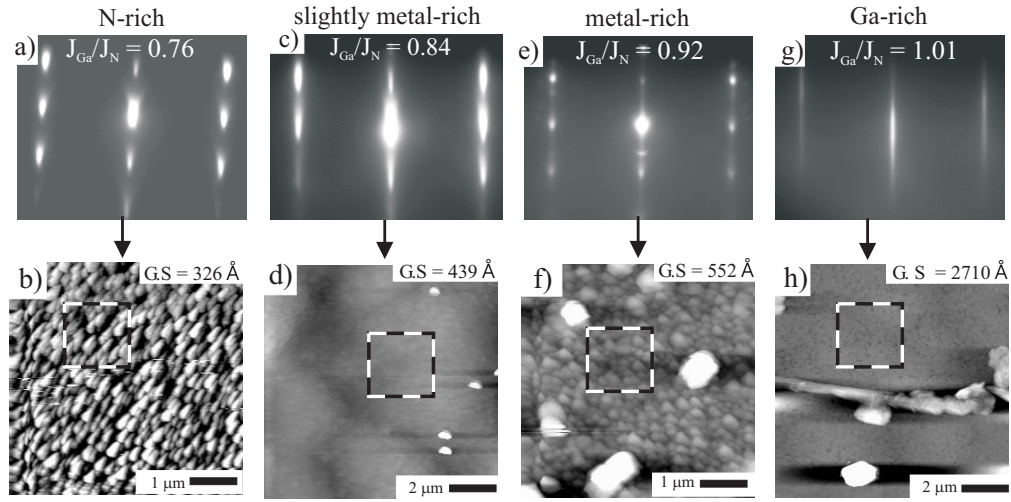


Fig. 1 RHEED patterns obtained during the growth and AFM images, obtained *ex situ* after the growth, of the MnGaN samples grown at different Ga/N flux ratios. gray scale(GS) is shown on the right hand corner of the AFM images.

shown that under N-rich growth, Mn is incorporated on the Ga lattice sites, but the de-channeling of 10% indicates defects, which could include some possible Mn and/or Ga interstitials.[10] The Ga-polarity of the lattice is maintained during MnGaN growth under N-rich conditions.[10] A schematic of the surface structure of N-rich MnGaN growth is shown in Fig. 2(a). For wurtzite GaN, the stacking sequence is ABABAB... If diffusion is limited, atoms may not find the correct site to maintain this sequence, which may result in stacking faults and other lattice defects. We note that, for the N-rich grown film, we did not observe any statistically significant change in the lateral or perpendicular lattice constants, which one might expect with interstitials. Therefore, the RBS de-channeling of 10% may be more likely attributed to stacking faults.

3.1.2 Slight Metal-rich Growth Mode

A qualitatively different mode of growth occurs when the Ga flux is increased to $R_{Ga:N} = 0.84$ (MnGaN-2), as shown in Figs. 1(c,d), which corresponds to slightly metal-rich growth. Although the RHEED pattern is only slightly less spotty as compared to N-rich growth, the $10 \mu\text{m} \times 10 \mu\text{m}$ AFM image (with gray scale of 439 Å and rms roughness of 12 Å inside the box area) shows a significantly smoother-looking surface than MnGaN-1 (N-rich). The few small dots appearing in the image of Fig. 1(d) are due to the slight excess of metal (Ga and/or Mn). For slight metal-rich growth, RBS has shown incorporation of Mn into the GaN lattice as well as increased channeling compared to N-rich growth, suggesting better crystallinity. The polarity for slight metal-rich growth of MnGaN is also maintained from the starting Ga-polarity of the substrate.[10] A schematic surface structure of the metal-rich grown MnGaN sample is shown in Fig. 2(b).

3.1.3 Metal-rich Growth Mode

Increasing the Ga flux to $R_{Ga:N} = 0.92$ (MnGaN-3) results in increased metal-rich conditions, as shown in Figs. 1(e,f). The RHEED pattern is more spotty, and the $5 \mu\text{m} \times 5 \mu\text{m}$ AFM image (with gray scale of 552 Å and rms roughness of 72 Å inside the box area) shows a rougher surface as well as an increased density of dots appearing on the surface. These dots are attributed to excess metal (Ga and/or Mn). In addition to the dots, we also found that, for highly metal-rich conditions, the polarity of the sample is reversed (from Ga-polar to N-polar).[10]

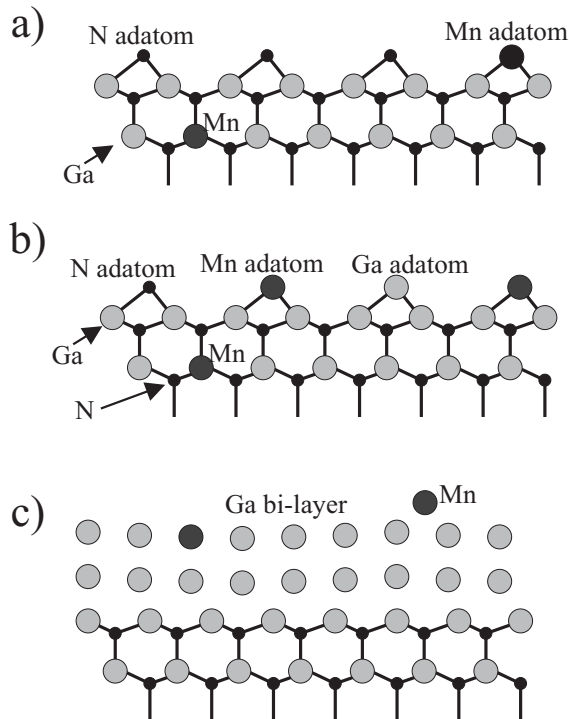


Fig. 2 Schematic of surface structural models for a) N-rich b) metal-rich and c) Ga-rich growth of MnGaN

3.1.4 Ga-rich Growth Mode

For Ga-rich growth conditions, the mode of growth is completely different. The RHEED pattern obtained during the growth of MnGaN (MnGaN-4) under Ga-rich conditions [$R_{Ga:N} = 1.01$] and subsequent AFM image are shown in Figs. 1(g,h). Clearly the RHEED pattern is streaky, indicating a smooth growth, and the $10 \mu\text{m} \times 10 \mu\text{m}$ AFM image (with gray scale of 2710 \AA and rms roughness of 41 \AA inside the box area) reveals the large smooth regions of the surface, similar to what is found for Ga-rich GaN growth.[9] Yet, some large dot-like as well as rod-like features are found at the surface. These are attributed to metal accumulation. Some of these (with rod-like shape) are up to hundreds of microns in length, whereas the dot-like features have lateral dimensions of only $2\text{-}10 \mu\text{m}$. According to energy dispersive x-ray spectroscopy (EDX), these accumulates contain large amounts of Mn, whereas the smooth areas of the surface contain very little if any Mn.[10] The mechanism behind this distinctly 2-phase growth mode has been explained previously as being caused by the existence of a double Ga layer on the surface, which is known for Ga-rich GaN(0001).[11] RBS of the Ga-rich grown sample shows high crystallinity but no evident Mn incorporation. No reversal of the lattice polarity was found for Ga-rich growth. A schematic diagram of the surface structure of the Ga-rich MnGaN growth is shown in Fig. 2(c).

3.2 Magnetic Properties of MnGaN as Functions of the Growth Modes

The 4 modes of growth just described lead to distinctly different magnetic properties as measured by SQUID magnetometry. The Mn incorporated was estimated from RBS measurements for samples MnGaN-1, MnGaN-2, and MnGaN-4 to be 5%, 5%, and 0% respectively. It should be noted that the uncertainty of these estimates is $\sim 2\%$. For MnGaN-3, RBS was not performed; we assume that the total amount of Mn is still 5% although some is in the form of accumulates. For Ga-rich (MnGaN-4) we assume the Mn is all in the Mn-rich accumulates which is approximately 5% of total metal. Therefore, in the following, the

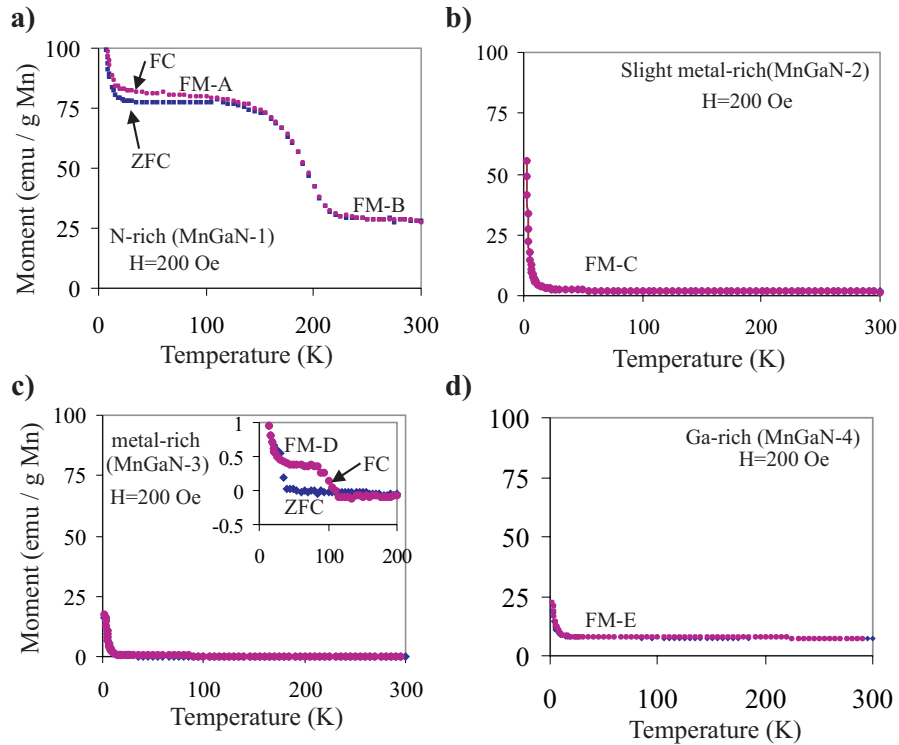


Fig. 3 Magnetization (emu per grams of Mn) as a function of temperature of MnGaN samples grown under N-rich, slight metal-rich, metal-rich, and Ga-rich growth regimes

magnetization/gMn were calculated for each film by estimating the total amount of Mn in the film as 5% of Ga, whether as incorporated or as accumulates.

Shown in Figs. 3(a-d) are plots of the temperature dependence of the field cooled (FC) and zero field cooled (ZFC) magnetization of the MnGaN samples for N-rich, slight metal-rich, metal-rich, and Ga-rich growth conditions. For all 4 cases, a low-temperature paramagnetic behavior becomes clearly apparent in the temperature range $T < 20\text{-}30\text{K}$.

Magnetization of the samples grown under N-rich, slight metal-rich, metal-rich and Ga-rich conditions is plotted as a function of applied field as shown in Figs. 4(a-d). A clear remnant magnetization can be seen in all 4 cases. Note that all the M-H loops were acquired at room temperature except for MnGaN-3, which was acquired at 30K. The coercive field in each case is also shown in Figs. 4(a-d).

3.2.1 Magnetic Properties: N-rich Growth

As seen in Fig. 3(a), in the case of N-rich growth (MnGaN-1) above about 20K, the magnetization becomes approximately constant (slowly decreasing for FC data) (~ 77 emu/g Mn at 200 Oe applied field) with temperature for both FC and ZFC curves up to $\sim 150\text{K}$. Since there is not too much difference between FC and ZFC data, evidently the applied field (200 Oe) is strong enough to rotate the moments even at low temperatures. The behavior suggests a ferromagnetic state (region FM-A) with a $T_C \approx 190\text{K}$. As temperature increases further, there is another region of nearly constant magnetization (~ 29 emu/gMn at 200 Oe applied field) in the range above 220K (region FM-B). This FM-B region has ferromagnetic behavior, and the T_C is clearly above room temperature.

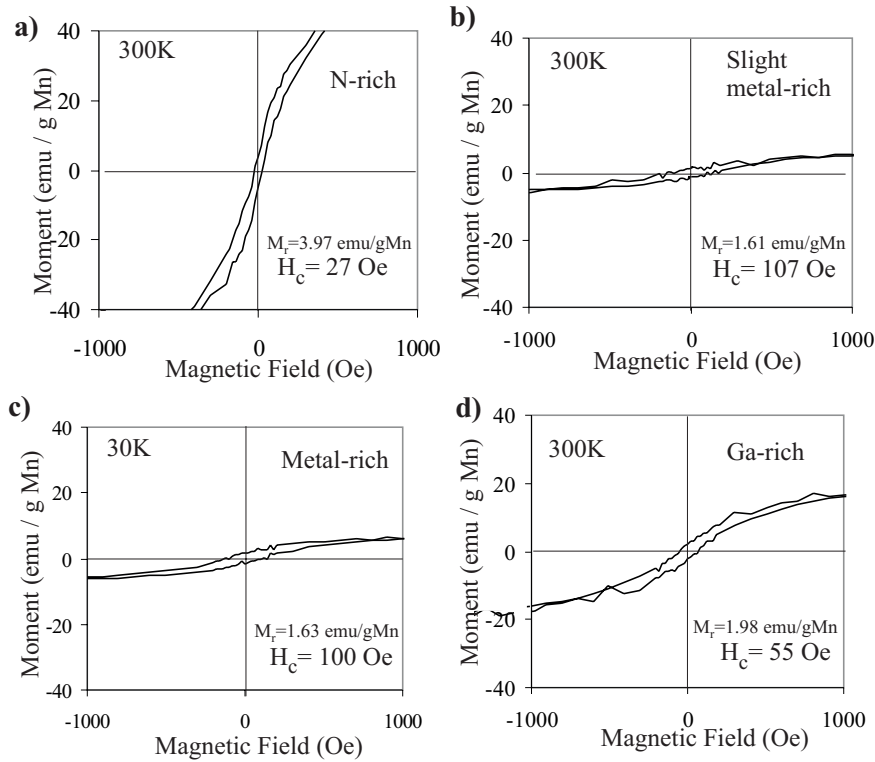


Fig. 4 Magnetization vs. magnetic field (hysteresis loops) of MnGaN samples grown under N-rich, slight metal-rich, metal-rich, and Ga-rich growth regimes

The magnetization vs. applied magnetic field (hysteresis loop) is plotted for MnGaN-1 in Fig. 4(a) for $T=300\text{K}$, which shows ferromagnetic behavior with a coercive field of $H_C = 27\text{ Oe}$. The magnetization reaches a value of $\sim 65\text{ emu/gMn}$ at 1000 Oe . Remnant magnetization of MnGaN-1 is 3.97 emu/gMn .

3.2.2 Magnetic Properties: Slight Metal-rich Growth

A qualitatively different magnetic result is found for a slightly metal-rich grown sample (MnGaN-2), as shown in Fig. 3(b). The ZFC and FC curves follow very closely to each other. After the paramagnetic transition there is only a single ferromagnetic region (FM-C) up to room temperature. Within the FM-C region, the magnetization is very low ($\sim 2.1\text{ emu/gMn}$ at 200 Oe applied field) although T_C is clearly above room temperature. This M vs. T curve is comparable to that reported in some earlier work.[5]

Shown in Fig. 4(b) is the M - H hysteresis curve for MnGaN-2 at $T=300\text{K}$. This sample shows a relatively large coercive field of 107 Oe but $\sim 13\times$ smaller magnetization (5.12 emu/gMn at 1000 Oe) compared to MnGaN-1 (N-rich). Remnant magnetization of slight metal-rich grown sample (MnGaN-2) is 1.61 emu/gMn .

3.2.3 Magnetic Properties: Metal-rich Growth

For the metal-rich grown sample (MnGaN-3), yet a different magnetic behavior is observed. As seen in Fig. 3(c) for the ZFC data, the magnetization drops sharply to nearly zero at $\sim 30\text{K}$. For the FC data, the paramagnetic region at the lowest temperatures gives way to a weak ferromagnetic region (FM-D) with a $T_C \sim 100\text{K}$, which can be seen more clearly in the inset shown in Fig. 3(c). We note that the magnetization

for the FM-D region (~ 0.37 emu/gMn at 200 Oe applied field) is more than 2 orders of magnitude smaller than that of the FM-A region of N-rich-grown sample MnGaN-1 and ~ 80 times smaller than that of the FM-B region of sample MnGaN-1. Above this weak FM-D region, the magnetization drops to nearly zero as with the ZFC data.

The hysteresis loop is plotted in Fig. 4(c) for MnGaN-3 at $T=30$ K. The coercive field at this temperature is relatively large (100 Oe) - about $4\times$ the value for MnGaN-1 (N-rich) at 300K. However, the magnetization is only ~ 5.82 emu/gMn at 1000 Oe applied field. Remnant magnetization of metal-rich grown sample (MnGaN-3) is 1.63 emu/gMn at 30K.

3.2.4 Magnetic Properties: Ga-rich Growth

Finally, the magnetic property of the Ga-rich grown sample (MnGaN-4) is yet again very different compared to those of MnGaN-1, MnGaN-2, and MnGaN-3, as seen in Fig. 3(d). Little difference is seen between FC and ZFC data for the given applied field (200 Oe). Above the paramagnetic region, from about 20K and up, the magnetization is approximately constant (but slowly decreasing) all the way up to room temperature. This ferromagnetic region, denoted FM-E, has a T_C clearly above room temperature. We note that the magnitude of the magnetization is ~ 7.85 emu/gMn (at 200 Oe applied field) in region FM-E.

The hysteresis loop for MnGaN-4 is shown in Fig. 4(d) for $T=300$ K. At this temperature, the coercive field is ~ 55 Oe, more than twice as large as that for MnGaN-1. Yet, the magnetization at 1000 Oe applied field is ~ 16.68 emu/gMn - about one fourth that of MnGaN-1. Remnant magnetization of Ga-rich grown sample (MnGaN-4) is 1.98 emu/gMn.

3.3 Interpretation of Magnetic Results and Correlation with Structural Properties

The results presented here show that for the 4 growth conditions studied, each corresponds to unique magnetic properties. Briefly, while the N-rich sample shows 2 magnetic regions with fairly large magnetization up to > 300 K, the metal-rich and slightly metal-rich samples have very small magnetizations. For the Ga-rich sample, the magnetization is much larger than for the metal-rich case. These different regions can be interpreted in terms of different origins of ferromagnetism.

For the N-rich (MnGaN-1) sample, the calculated average magnetic moment per Mn atom at 300K is $1.13 \mu_B$. Below 190K, the average magnetic moment increases to $\sim 1.85 \mu_B$. These calculated average magnetic moments/Mn atom are smaller than the theoretical value of $3.5 \mu_B$ per Mn ion in MnGaN predicted by Das *et al.*[12] and also much smaller than the theoretical values for the Mn site in Mn_xN clusters calculated by Rao *et al.* which range from $4.12-4.54 \mu_B$. [13]. One explanation could be that the number of Mn which are magnetically active is much less than the total number of Mn in the sample.

Shown in Fig. 5 is a plot of the remnant magnetization of MnGaN-1 versus temperature. For comparison, zero-field cooled data of MnGaN-1 is also shown in the graph. The remnant magnetization values are taken from hysteresis measurements which were obtained at different temperatures: 5K, 30K, 180K, and 300K. The trend of the remnant magnetization values at 30K, 180K, and 300K matches very well with the trend of the ZFC data. However, while the ZFC magnetization increases, the remnant magnetization decreases, as temperature decreases towards 5K. It is interesting to note that this kind of drop off in the remnant magnetization was not observed in other samples grown under different growth modes.

As described previously, the N-rich sample has two ferromagnetic components as is evident from ZFC and FC data. One of the components (FM-B) has T_C above room temperature, and the other (FM-A) has T_C around 190K. To explain this behavior of the remnant magnetization, we consider that the magnetism is due to either large magnetic accumulates, small magnetic nano-clusters, or else magnetic ions (e.g. carrier-mediated ferromagnetism). If we rule out the accumulates based on the fact that none were seen on the N-rich growth surface, that leaves 2 possibilities. In the case of clusters, there would need to be 2 different types to explain the 2 regions FM-A and FM-B. This is certainly possible.[13] Still, the question

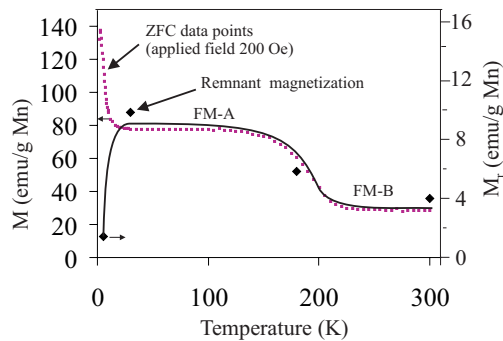


Fig. 5 Remnant magnetization and zero field cooled data as a function of temperature of N-rich MnGaN-1 sample. Solid curve is a guide to the eye.

is how could the remnant magnetization drop off to a value at 5K below the values at 30K and 300K? Such behavior for magnetic clusters has in fact been reported in the paper by Ploog *et al.*[14] But on the other hand, Ploog *et al.* have not observed a feature similar to the FM-A region shown here. In addition, so far we have no direct imaging or observation of such clusters in this sample. Future studies with TEM would be useful to look for clusters.

The other possibility is that the ferromagnetism is due to isolated magnetic ions whose magnetic moments are aligned by mediating carriers (carrier-mediated ferromagnetism). To check the electronic properties of this N-rich grown sample, we performed resistivity measurements over the temperature range from 350K down to 77K. We found that the resistivity of MnGaN-1 (grown N-rich) is very small - about .008 ohm-cm - and is almost constant throughout the temperature range. We also found out that MnGaN-1 is *n*-type. This suggests that MnGaN-1 has a high density of extrinsic conduction electrons. Therefore, these results support the possibility of a carrier-mediated ferromagnetism in this sample.

The drop-off of remnant magnetization below 20K could be attributed to carrier freeze-out. Then the magnetic moments of the Mn ions will be oriented randomly, and the sample will become paramagnetic. However, it is challenging to explain both ferromagnetic regions (FM-A and FM-B) having different T_C 's as both being carrier-mediated (although that might be possible if there existed 2 different types of magnetic species).

Third possible explanation is that the magnetic behavior of N-rich grown MnGaN-1 is a combination of carrier-mediated ferromagnetism (region FM-A) and ferromagnetic clusters (region FM-B). This is reasonable since the Curie temperature of large ferromagnetic clusters is expected to be much greater than 300K.[13] Moreover, if we compare the ZFC/FC measurements of MnGaN-1 with the results of Ploog *et al.*, it is evident that FM-A region is not observed in either of their samples, while FM-B region appears more like the magnetic results of their sample B, which was attributed to ferromagnetic clusters.[14] In addition, Ploog *et al.* reported that their samples were insulating, whereas MnGaN-1 sample was found to be conducting. In the future, it would be useful to vary the Mn concentration and look for changes in the T_C of the FM-A region.

For the case of slight metal-rich growth conditions (MnGaN-2), the magnetic moment per Mn atom was calculated to be only about $0.084 \mu_B$ at 300K. This very small value indicates that either very few of the Mn are magnetically active and/or there are significant antiferromagnetic interactions. The slight metal-rich regime has the advantage of avoiding the polarity reversal of metal-rich growth; the material remains Ga-polar. But although Mn is incorporated on Ga lattice sites as determined by RBS,[10] and there are very few and small metallic particles, large magnetic moments are still not achieved.

For the metal-rich conditions (MnGaN-3), the calculated magnetic moment per Mn atom in this film is only $0.082 \mu_B$ at 30K. It suggests that few of the Mn are magnetically active and/or there are significant

antiferromagnetic interactions. In any case, the metal termination of the surface in metal-rich growth can provide for some reasonable amount of diffusion on the surface. Mn is incorporated in the lattice, although some metallic accumulates are observed. Despite the likely Mn incorporation, a large magnetic moment is not achieved.

For the Ga-rich growth (MnGaN-4), the average magnetic moment/Mn atom is $0.23 \mu_B$ at 300K. Although the T_C is above room temperature and the magnetic moment is larger than for metal-rich case, the magnetism can be attributed to metallic ferromagnetic accumulates,[15] which are shown in the AFM image [Fig. 1(h)]. Energy dispersive x-ray (EDX) analysis has previously shown that these accumulates contain significant concentrations of Mn.[10] They may be composed of ferromagnetic Mn_xGa_y compounds as well as ferrimagnetic Mn_4N , both of which have critical temperatures greater than room temperature. The origin of the ferromagnetic accumulation in Ga-rich conditions can be attributed to the presence of a double layer of Ga on Ga-polar GaN(0001) in Ga-rich conditions.[10, 11] This highly mobile layer can promote the fast diffusion and accumulation of Mn. Fast diffusion is consistent with the high crystalline quality of the Ga-rich grown film, but Mn is not incorporated into the lattice substitutionally.

4 Conclusion and Outlook

It has been shown that the magnetic properties of the MnGaN samples strongly depend on the growth mode. N-rich growth results in two fairly large magnetic components, one of which has a transition temperature which exceeds 300K and the other is at ~ 190 K. Slight metal-rich growth results in a single very small magnetic component with transition above 300K. Metal-rich growth results in a film with almost zero magnetization at 300K. Finally, Ga-rich growth results in a significant magnetization which is attributed to Mn_xGa_y or Mn_4N compounds. None of the samples discussed here had average values of magnetic moment as large as the theoretical predictions for Mn in GaN.

For DMS behavior, the most likely region based on this study is the N-rich growth regime where a significant magnetic moment is observed. Under N-rich conditions, ferromagnetic metal accumulation and polarity reversal are avoided. The magnetic results for the N-rich grown sample are interpreted as a combination of carrier-mediated ferromagnetism with $T_C \sim 190$ K and ferromagnetic clusters with T_C much greater than room temperature. Further studies are needed to verify the possibility of carrier-mediated ferromagnetism in this sample. For slight metal-rich and metal-rich growth, accumulates are observed although the magnetizations measured for these samples were very small; so, these accumulates do not appear to be ferromagnetic. For Ga-rich growth, the observed ferromagnetism is attributed to the properties of ferromagnetic Mn-rich accumulates which are clearly visible at the surface.

Acknowledgements This material is based upon work supported by the National Science Foundation under grant Nos. 9983816 and 0304314.

References

- [1] H. Ohno, *Science* **281**, 951 (1998).
- [2] K. Sato, and H. Katayama-Yoshida, *Semicond. Sci. Technol.* **17**, 367 (2002).
- [3] S. Sonoda, S. Shimizu, T. Sasaki, Y. Yamamoto, and H. Hori, *J. Cryst. Growth* **237-239**, 1358 (2002).
- [4] M. L. Reed, N. A. El-Masry, H. H. Stadelmaier, M. K. Ritums, M. J. Reed, C. A. Parker, J. C. Roberts and S. M. Bedair, *Appl. Phys. Lett.* **79**, 3473 (2001).
- [5] G. T. Thaler, M. E. Overberg, B. Gilla, R. Frazier, C. R. Abernathy, S. J. Pearton, J. S. Lee, S. Y. Lee, Y. d. Park, Z. G. Khim, J. Kim, and F. Ren, *Appl. Phys. Lett.* **80**, 3964 (2002).
- [6] M. E. Overberg, C. R. Abernathy, S. J. Pearton, N. A. Theodoropoulou, K. T. McCarthy, and A. F. Hebard, *Appl. Phys. Lett.* **79**, 1312 (2001).
- [7] R. Held, D. E. Crawford, A. M. Johnson, A. M. Dabiran, and P. I. Cohen, *J. Electron. Mater.* **26**, 272 (1997).
- [8] E. J. Tarsa, B. Heying, X. H. Wu, P. Fini, S. P. DenBaars, and J. S. Speck, *J. Appl. Phys.* **82**, 5472 (1997).

- [9] R. M. Feenstra, H. Chen, V. Ramachandran, C. D. Lee, A. R. Smith, J. E. Northrup, T. Zywietz, J. Neugebauer, and D. W. Greve, *Surface Rev. Lett.* **7**, 601 (2000).
- [10] M. B. Haider, C. Constantin, H. Al-Britthen, H. Yang, E. Trifan, D. Ingram, A. R. Smith, C. V. Kelly and Y. Ijiri, *J. Appl. Phys.* **93**, 5274 (2003).
- [11] A. R. Smith, R. M. Feenstra, D. W. Greve, M.-S. Shin, M. Showronski, J. Neugebauer, and J. E. Northrup, *Surf. Sci.* **423**, 70 (1999).
- [12] G. P. Das, B. K. Rao, and P. Jena, *Phys. Rev. B*, **68**, 035207-1(2003)
- [13] B. K. Rao, and P. Jena, *Phys. Rev. Lett.*, **89**, 185504-1(2004)
- [14] K. H. Ploog, S. Dhar, and A. Trampert, *J. Vac. Sci. Technol. B* **21**(4), 1756(2003)
- [15] M. Tanaka, J. P. Harbison, T. Sands, B. Philips, T. L. Cheeks, J. De. Boeck, L. T. Florez, and V. G. Keramidas, *Appl. Phys. Lett.*, **63**, 696(1993)